



UvA-DARE (Digital Academic Repository)

Fast and slow sound in the two-temperature model

Schram, R.P.C.; Wegdam, G.H.

DOI

[10.1016/0378-4371\(94\)90030-2](https://doi.org/10.1016/0378-4371(94)90030-2)

Publication date

1994

Published in

Physica A : Statistical Mechanics and its Applications

[Link to publication](#)

Citation for published version (APA):

Schram, R. P. C., & Wegdam, G. H. (1994). Fast and slow sound in the two-temperature model. *Physica A : Statistical Mechanics and its Applications*, 203, 33-52.
[https://doi.org/10.1016/0378-4371\(94\)90030-2](https://doi.org/10.1016/0378-4371(94)90030-2)

General rights

It is not permitted to download or to forward/distribute the text or part of it without the consent of the author(s) and/or copyright holder(s), other than for strictly personal, individual use, unless the work is under an open content license (like Creative Commons).

Disclaimer/Complaints regulations

If you believe that digital publication of certain material infringes any of your rights or (privacy) interests, please let the Library know, stating your reasons. In case of a legitimate complaint, the Library will make the material inaccessible and/or remove it from the website. Please Ask the Library: <https://uba.uva.nl/en/contact>, or a letter to: Library of the University of Amsterdam, Secretariat, Singel 425, 1012 WP Amsterdam, The Netherlands. You will be contacted as soon as possible.

Fast and slow sound in the two-temperature model

R.P.C. Schram and G.H. Wegdam

*Van der Waals-Zeeman Laboratory, University of Amsterdam, Valckenierstraat 65,
1018XE Amsterdam, The Netherlands*

Received 21 June 1993

The dispersion relation for disparate mass gas mixtures is derived from a simplified two-temperature model. It is shown that the hydrodynamic sound mode ($kl \rightarrow 0$) goes over continuously into either a fast or a slow propagating sound mode ($kl \rightarrow \infty$), depending on the composition. The composition that demarcates the composition regions where the continuation of the hydrodynamic sound mode is a fast or slow propagating mode is called the critical composition. The existence of such a critical composition is confirmed experimentally by new Rayleigh–Brillouin experiments on $H_2 + Xe$ mixtures.

1. Introduction

In a number of recent studies a fast propagating collective mode was shown to exist in high- and low-density disparate mass mixtures [1–10]. The fast sound mode appears outside the hydrodynamic regime and has a propagation velocity which is much higher than that of the hydrodynamic sound mode. This new phenomenon is associated with dynamic decoupling of the light and heavy component at short length scales.

The renewed interest in the dynamics of disparate mass fluids was initiated by the work of Bosse et al. [1]. They observed a new high frequency peak in the selfstructure factor $S_{LiLi}(k, \omega)$ in a computer simulation of liquid $Li_{0.8}Pb_{0.2}$. This peak was associated with the collective Li density fluctuations and was named ‘fast sound’. The results were discussed within the framework of the Mori–Zwanzig formalism. At small wavenumbers the hydrodynamic sound mode and a zero-frequency diffusion eigenmode are predicted. At larger values of the wavevector a non-overdamped high-frequency collective mode appears that was interpreted as the rapid Li-density fluctuations in a background of heavy lead ions.

Campa and Cohen predicted the existence of a fast sound mode in dilute binary gas mixtures [2] and binary fluid mixtures [3,4], using revised Enskog theory. At small wavenumbers the usual hydrodynamic sound mode was found. At larger wavenumbers the calculations predict a fast propagating sound mode, which has a propagation velocity close to the sound velocity of the light component. The fast sound mode can either appear as an extension of the hydrodynamic sound mode or as a kinetic mode. Calculations of the selfstructure factors showed that this fast propagating collective mode is mainly carried by the light particles.

Experimentally, fast sound was observed in a dense He + Ne mixture by neutron scattering [5]. Using Rayleigh–Brillouin light scattering, slow sound was observed in dilute He + Xe mixtures [6]. Both fast and slow sound modes were observed in gaseous H₂ + Xe and H₂ + Ar mixtures using light-scattering [7–9]. Independently, Clouter et al. confirmed the existence of fast sound in H₂ + Ar and slow sound in H₂ + SF₆ [10].

Earlier, ultrasonic measurements indicated the existence of similar dynamic decoupling effects in disparate mass gas mixtures. Bowler and Johnson [11] performed these measurements on gaseous He + Xe mixtures. In these experiments both the velocity and the absorption of the ultrasonic waves are measured as a function of the frequency to pressure ratio. They found that the experimental dispersion relation of the acoustic mode changes dramatically when x_{He} (He-mole fraction) ≈ 0.5 . This was confirmed by two-temperature model calculations [11] and the calculations of Kamgar-Parsi and Cohen [12]. These models predict the existence of a ‘critical point’, at which the acoustic mode and a diffusive-type mode are degenerate. The dramatic change in the experimental dispersion relation of the acoustic mode was attributed to mode interference of a diffusive-type mode and the acoustic mode. Bowler and Johnson [11] used a simplified version of the two-temperature model, the four moment model, to describe their ultrasonic experiments on dilute gas mixtures. This simple model provided a good estimate of some characteristic features of the experimental dispersion relation. For example, the four moment model predicts a ‘critical composition’ of $x_{\text{He}} = 0.5$, which is in good agreement with experiment and the predictions of the more complicated ten moment model [11,12].

In this paper we will present the four moment model and the six moment model for gas mixtures and compare these models with the results of our light scattering experiments. Both models are simplified versions of the full two-temperature model, which incorporates 26 moments [13]. We will study the dispersion relation of both models, in a similar way as earlier studies of sound propagation gaps in pure fluids [14], gas mixtures [15] and double sound propagation in gas mixtures [16]. Although the four moment model does not

include temperature fluctuations, it is useful since many of the two-temperature characteristics can be obtained analytically. The six moment model contains the main characteristics of the more elaborate hydrodynamic or kinetic models. Moreover, it describes qualitatively the experimental dispersion relations of the fast and slow sound mode in binary gas mixtures. Although there are quantitative discrepancies between model and experiment, the main advantage of the simplified approach is that there are no adjustable parameters involved and it offers a useful physical picture. Both models predict dynamic decoupling of the light and heavy component at short length scales as well as the existence of two dynamic regions in the composition. These composition regions are characterized by domination of the dynamics of the light or the heavy particles and are separated by a ‘critical composition’. The existence of such a composition is confirmed qualitatively by new experiments on $H_2 + Xe$ mixtures.

This paper is organized as follows: In section 2 the theory of the simplified two-temperature models will be discussed. The dispersion relation and its ‘critical behaviour’ will be derived. A comparison with experimental results will be given in section 3. Discussion and conclusion can be found in sections 4 and 5.

2. Theory

The following theory is based on the moments of the species velocity distribution function f_i [17]. The basic equations of the full two-temperature model (26 moments) can be found in ref. [13]. The predictions of the ten moment model for ultrasonic experiments are given by Kamgar-Parsi and Cohen [12] and Bowler and Johnson [11]. These 10 moments correspond to the number densities, flow velocities, temperatures, heat fluxes and pressure tensors of both species. In the following derivation of the dispersion relation we will essentially follow the notation of ref. [11]. In the present approach only six moments will be considered:

$$n_i = \int dc_i f_i, \tag{1}$$

$$n_i \mathbf{u}_i = \int dc_i c_i f_i, \tag{2}$$

$$3n_i k_B T_i = \int dc_i m_i c_i^2 f_i, \tag{3}$$

where n_i , \mathbf{u}_i and T_i are the number density, the flow velocity and the temperature of species i , k_B is the Boltzmann constant and m_i is the mass of particle i . The integrations are performed with respect to \mathbf{c}_i ($= \boldsymbol{\xi}_i - \mathbf{u}_i$), the peculiar velocity of a particle of type i , where $\boldsymbol{\xi}_i$ is a molecular velocity. The subscript $i = 1, 2$ denotes the light and heavy component, respectively. Using the Boltzmann equation (external forces are not considered here):

$$\frac{\partial f_i}{\partial t} + \boldsymbol{\xi}_i \cdot \nabla f_i = \left[\frac{df_i}{dt} \right]_{\text{collision}}, \quad (4)$$

the linearized dynamic equations for the moments can be obtained [17]:

$$\frac{\partial n_i}{\partial t} + n_{i0} \nabla \cdot \mathbf{u}_i = 0, \quad (5)$$

$$\rho_{i0} \frac{\partial \mathbf{u}_i}{\partial t} + \nabla p_i = K_{ij} (\mathbf{u}_j - \mathbf{u}_i), \quad (6)$$

$$\frac{3}{2} n_{i0} k_B \frac{\partial T_i}{\partial t} + p_{i0} \nabla \cdot \mathbf{u}_i = 3 \frac{K_{ij}}{(m_1 + m_2)} k_B (T_j - T_i), \quad i \neq j, \quad (7)$$

where the partial pressure $p_i = n_i k_B T_i$ and ρ_i ($= m_i n_i$) is the mass density of species i . The subscript 0 denotes an equilibrium value. The parameter $K_{ij} = A \rho_{i0} \rho_{j0}$ [17] can be calculated for any given interaction potential. It can also be approximated by a phenomenological model of gas mixture in which diffusion is the only relaxation process [11]. In that case A is related to the diffusion coefficient D by

$$A = \frac{k_B T_0}{n_0 m_1 m_2 D}, \quad (8)$$

where n_0 is equilibrium value of the total number density ($= n_{10} + n_{20}$). For hard sphere mixtures A can be calculated exactly and is given by

$$A = \frac{8}{3} \frac{\sqrt{\pi} \sigma_{12}^2}{(m_1 + m_2)} W, \quad (9)$$

where the reference speed $W = (2k_B T_0 / \mu)^{1/2}$, μ is the reduced mass, $\sigma_{12} = (\sigma_1 + \sigma_2)/2$ and σ_i is the hard-sphere diameter of species i .

We will use the following set of variables: the number densities n_i ($i = 1, 2$), the overall flow velocity $\mathbf{u} = \zeta_1 \mathbf{u}_1 + \zeta_2 \mathbf{u}_2$, the diffusion velocity $\mathbf{w} = \mathbf{u}_1 - \mathbf{u}_2$, the overall temperature $T = x_1 T_1 + x_2 T_2$ and the temperature difference $\Delta = T_1 - T_2$, where $x_i = n_{i0} / n_0$ and $\zeta_i = \rho_{i0} / \rho_0$ are the mole fraction and the mass

fraction of species i , respectively. Since we are mainly interested in longitudinal sound modes, we will consider only the longitudinal part of the variables, parallel to the wavevector \mathbf{k} (the x -direction). The nondimensional form of these variables is defined by

$$n_i = n_{i0} \hat{n}_i e^{i\theta}, \quad (10)$$

$$u = W \hat{u} e^{i\theta}, \quad (11)$$

$$w = W \hat{w} e^{i\theta}, \quad (12)$$

$$T = T_0 \hat{T} e^{i\theta}, \quad (13)$$

$$\Delta = T_0 \hat{\Delta} e^{i\theta}, \quad (14)$$

where $\theta = kx - \omega t$, k is the length of the wavevector \mathbf{k} , ω is the angular frequency and \hat{a} denotes the complex (dimensionless) amplitude of the quantity a . We will define the reference frequency ν and the reference length scale l by:

$$\nu = A(m_1 + m_2)n_0, \quad (15)$$

$$l = W/\nu. \quad (16)$$

If eqs. (10)–(14) are inserted in eqs. (5)–(7), one obtains

$$z^* \hat{n}_1 + ikl(\hat{u} + \zeta_2 \hat{w}) = 0, \quad (17)$$

$$z^* \hat{n}_2 + ikl(\hat{u} - \zeta_1 \hat{w}) = 0, \quad (18)$$

$$z^* \hat{u} + ikl \frac{1}{2} \frac{m_{10} m_{20}}{m_{12}} (x_1 \hat{n}_1 + x_2 \hat{n}_2) = 0, \quad (19)$$

$$z^* \hat{w} + ikl \frac{1}{2} m_{10} m_{20} \left(\frac{\hat{n}_1}{m_{10}} - \frac{\hat{n}_2}{m_{20}} + \left(\frac{1}{m_{10}} - \frac{1}{m_{20}} \right) \hat{T} + m_{12} \Delta \right) = -m_{12} \hat{w}, \quad (20)$$

$$z^* \hat{T} + ikl \frac{2}{3} \left(\hat{u} + \frac{m_{20} - m_{10}}{m_{12}} x_1 x_2 \hat{w} \right) = 0, \quad (21)$$

$$z^* \hat{\Delta} + ikl \frac{2}{3} \hat{w} = -2m_{10} m_{20} \Delta, \quad (22)$$

where $z^* = z/\nu$, with $z = -i\omega$ and $m_{i0} = m_i/(m_1 + m_2)$. The right hand terms of eqs. (20) and (22) account for the coupling between the light and heavy subsystem. These terms originate from the transferintegrals for momentum and kinetic energy, respectively. As can be seen in eqs. (6) and (7), momentum and kinetic energy are transferred only by i - j collisions ($i \neq j$). Thus, in the present approach the dynamics of the light and heavy subsystem are coupled by the species flow velocities and species temperatures.

We will now consider only four moments (eqs. (17)–(20)); the temperature fluctuations will be neglected. This is a two-velocity model to which we will refer as the four moment model. The dispersion relation for the model reads

$$\tilde{z}^4 + \frac{m_{12}}{kl} \tilde{z}^3 + \frac{1}{2} \tilde{z}^2 + \frac{\alpha^2}{2kl} \tilde{z} + \frac{1}{4} \alpha^2 = 0, \quad (23)$$

with $\tilde{z} = z/Wk$, $\alpha^2 = m_{10}m_{20}$ and $m_{12} = x_1m_{10} + x_2m_{20}$. The scaled dispersion relation has only three independent parameters: the reduced wavevector kl , the mass ratio m_2/m_1 and the heavy component mole fraction x_2 . Note that we used two differently scaled eigenvalues, \tilde{z} and z^* , which are related by $\tilde{z} = z^*/kl$. The scaling of \tilde{z} is more convenient for comparison with the experimental results (section 3).

A plot of the dispersion relation is given in fig. 1 for two compositions. In the limit $kl \rightarrow 0$ the eigenvalues of the diffusive-type modes are

$$z = -Dk^2, \quad (24)$$

$$z = -\nu_w + \mathcal{O}(k^2), \quad (25)$$

with $\nu_w = m_{12}\nu$. The first mode is the particle diffusion mode, the second mode is associated with the relaxation of the diffusion velocity w . In addition to these two purely damped modes, two propagating modes are found:

$$z = \pm ic_T k + \mathcal{O}(k^2). \quad (26)$$

Since we neglected the temperature fluctuations in the present approach, we do not find the usual adiabatic sound velocity for the phase velocity of these ‘hydrodynamic’ sound modes but instead we find $c_T = \sqrt{k_B T_0 / (m_1 x_1 + m_2 x_2)}$, which is the isothermal sound velocity of an ideal gas mixture.

In the limit of $kl \rightarrow \infty$ four propagating sound modes are found:

$$z = \pm ic_{T,1} k + \mathcal{O}(1), \quad (27)$$

$$z = \pm ic_{T,2} k + \mathcal{O}(1), \quad (28)$$

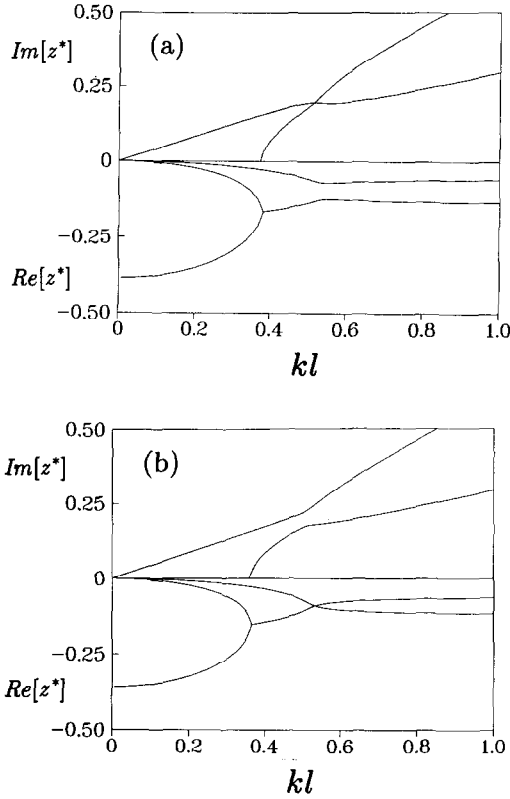


Fig. 1. Dispersion relation z^* ($= z/\nu$ versus kl (eq. (23), four moment model) for a mixture with mass ratio 5. (a) $x_2 = 0.33$, (b) $x_2 = 0.29$.

where $c_{T,i}$ ($= \sqrt{k_B T_0 / m_i}$) is the isothermal sound velocity of species i . These four modes represent isothermal waves propagating with the sound velocity of the pure component, as if the other component were not present. This suggests decoupling of the dynamics of the light and heavy component at short length scales ($kl \rightarrow \infty$).

At intermediate length scales some interesting features of the dispersion relation are obtained. As can be seen in fig. 1a, the two diffusive-type modes (eqs. (24) and (25)) merge into the fast propagating sound mode ($z = \pm ic_{T,1}k$). In the same kl -range the hydrodynamic sound mode ($z = \pm ic_T k$) goes over continuously into the slow propagating sound mode ($z = \pm ic_{T,2}k$). At a slightly lower concentration of the heavy component the situation is reversed (fig. 1b). Now the extension of the hydrodynamic sound mode is the fast propagating mode. Whether the extension of the hydrodynamic sound mode is a fast or slow propagating mode is thus found to depend on the composition. It is

therefore useful to define a ‘critical composition’ $x_{2,\text{crit}}$ that demarcates the regions of fast and slow continuation of the hydrodynamic sound mode. The existence of such a critical composition was already mentioned by Campa and Cohen [18]. At the ‘critical point’ the modes are two-fold degenerate so that the dispersion relation should be of the following form:

$$(\tilde{z} - \tilde{z}_{\text{crit}})^2(\tilde{z} - \overline{\tilde{z}_{\text{crit}}})^2 = 0, \quad (29)$$

where \tilde{z}_{crit} is the root of eq. (23) at the critical point. The coefficients of eq. (29) and eq. (23) equal when $m_{12} = \alpha$ and

$$x_{2,\text{crit}} = \frac{\delta}{1 + \delta}, \quad (30)$$

$$(kl)_{\text{crit}} = \frac{\alpha}{\sqrt{2(1 - 2\alpha)}}, \quad (31)$$

where $\delta^2 = m_1/m_2$. These critical parameters only depend on the mass ratio. The eigenvalues at the critical point are

$$\tilde{z}_{\text{crit}} = -\frac{1}{4}\sqrt{2(1 - 2\alpha)}\left(1 \pm \sqrt{\frac{1 - 6\alpha}{1 - 2\alpha}}\right), \quad 0 < \alpha \leq \frac{1}{6}, \quad (32)$$

$$\tilde{z}_{\text{crit}} = -\frac{1}{4}\sqrt{2(1 - 2\alpha)} \pm i\sqrt{\frac{1}{8}\left(\alpha - \frac{1}{6}\right)}, \quad \frac{1}{6} < \alpha \leq \frac{1}{2}. \quad (33)$$

For $0 < \alpha \leq \frac{1}{6}$, that is for $m_2/m_1 \geq 17 + 12\sqrt{2}$ (≈ 34), the imaginary part of \tilde{z}_{crit} equals zero, meaning that a sound propagation gap occurs at the critical point. This is demonstrated in fig. 2a, b for mass ratios smaller and larger than 34. As was shown in earlier papers, sound propagation gaps occur when the dissipative forces exceed the elastic forces [15,19].

At this point it is interesting to compare these results with the conditions for a sound propagation gap according to a simplified hydrodynamic model for mixtures [20,21]. In that hydrodynamic model viscosity and heat conduction are neglected; only diffusion is considered. It can be shown [15] that sound propagation gaps can occur only when

$$\gamma x_1 x_2 \frac{(\delta^2 - 1)^2}{(\delta^2 x_1 + x_2)^2} > 8, \quad (34)$$

where γ is the specific heat capacity ratio. The function at the left hand side of this inequality is proportional to the Brillouin width and has a maximum at

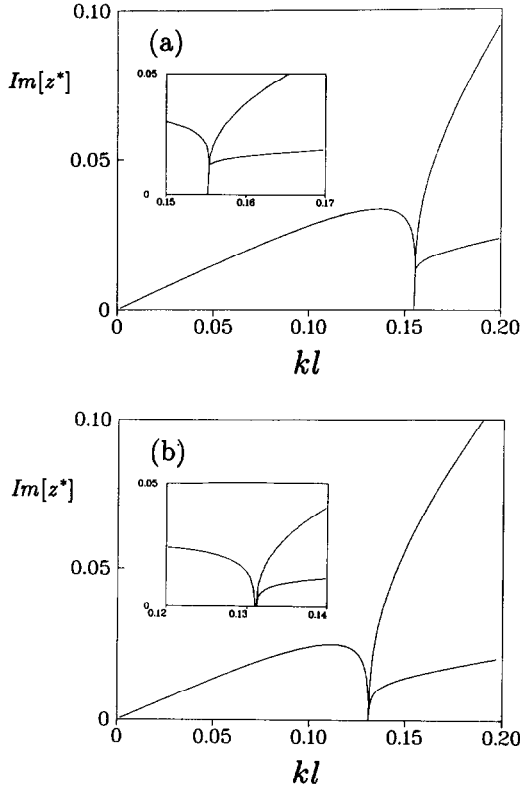


Fig. 2. Dispersion relation z^* versus kl (eq. (23), four moment model) for a mixture with critical composition. (a) $m_2/m_1 = 30$, (b) $m_2/m_1 = 40$.

$x_2 = \delta^2 / (1 + \delta^2)$. If this value of x_2 is inserted in eq. (34) we find that the condition for sound propagation gaps to occur is

$$\frac{m_2}{m_1} \geq \left(1 + \frac{16}{\gamma}\right) + 2\sqrt{\frac{8}{\gamma}\left(1 + \frac{8}{\gamma}\right)}. \quad (35)$$

If temperature fluctuations are neglected ($\gamma = 1$), we find the condition reduces to the simple relation

$$\frac{m_2}{m_1} \geq 17 + 12\sqrt{2}. \quad (36)$$

This is exactly the same condition for sound propagation gaps as was found for the present four moment model. The composition and the reduced wavevector

are different than the results found in eqs. (30) and (31), however. The basic equations of both models are different; the simplified hydrodynamic model uses only three hydrodynamic variables: density, concentration and flow velocity, while in the four moment model the diffusion velocity is incorporated as well. Apparently, the inclusion of the diffusion velocity does not affect the condition for a sound propagation gap in an isothermal ideal gas mixture.

In order to obtain the correct hydrodynamic limit we will now consider the simplified two-temperature model which will be referred to as the six moment model. When the temperature fluctuations are included the following dispersion relation can be calculated from eqs. (17)–(22):

$$\tilde{z} \left[\tilde{z}^5 + \frac{(2\alpha^2 + m_{12})}{kl} \tilde{z}^4 + \left(\frac{5}{6} + \frac{2\alpha^2 m_{12}}{(kl)^2} \right) \tilde{z}^3 + \frac{1}{6} \frac{\alpha^2}{kl} (15 - 4m_{12}) \tilde{z}^2 + \frac{5}{36} \alpha^2 \left(5 + \frac{12\alpha^2}{(kl)^2} \right) \tilde{z} + \frac{5}{6} \frac{\alpha^4}{kl} \right] = 0. \quad (37)$$

A plot of this dispersion relation is shown in fig. 3. As can be seen from eq. (37) one of the modes has the eigenvalue $z = 0$ for all values of kl . In the limit $kl \rightarrow 0$ the eigenvalues of the other five modes are

$$z = \pm ic_s k + \mathcal{O}(k^2), \quad (38)$$

$$z = -Dk^2, \quad (39)$$

$$z = -\nu_w + \mathcal{O}(k^2), \quad (40)$$

$$z = -\nu_\Delta + \mathcal{O}(k^2), \quad (41)$$

with $\nu_\Delta = 2\alpha^2\nu$. Contrary to the results of the four moment model, the correct adiabatic sound velocity $c_s = \sqrt{\frac{5}{3}}c_T$ for the sound modes is obtained (eq. (38)). The particle diffusion mode and diffusion velocity mode (eqs. (39) and (40)) were also found in the four moment model. In addition, a diffusive-type mode is found which is associated with the relaxation of the temperature difference (eq. (41)).

In the limit of $kl \rightarrow \infty$ the eigenvalues of the propagating modes are

$$z = \pm ic_{s,1} k + \mathcal{O}(1), \quad (42)$$

$$z = \pm ic_{s,2} k + \mathcal{O}(1). \quad (43)$$

These decoupled sound modes are propagating with the adiabatic sound velocity of the pure component $c_{s,i} = \sqrt{\frac{5}{3}}c_{T,i}$.

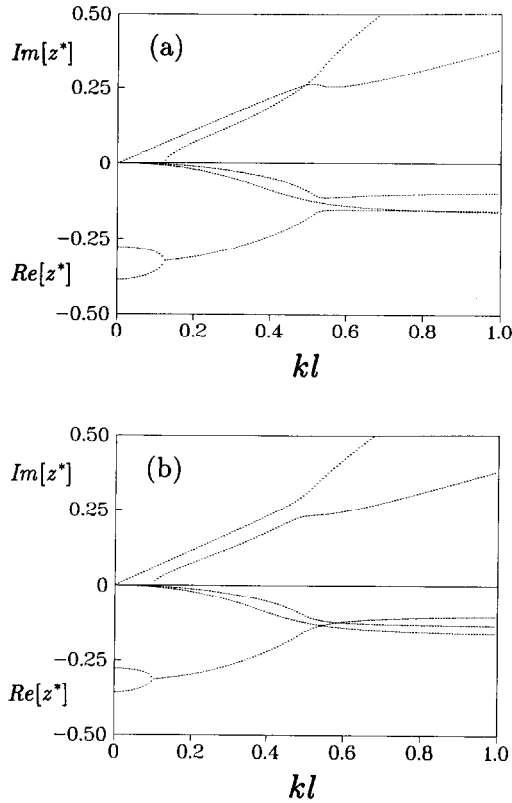


Fig. 3. Dispersion relation z^* versus kl (eq. (37), six moment model) for a mixture with mass ratio 5. (a) $x_2 = 0.33$, (b) $x_2 = 0.29$.

In the intermediate regime ($kl \sim 1$) one can still determine a critical composition within the six moment model although this cannot be done analytically.

The predictions for the critical compositions of both models are given in table I and fig. 4a. The results for the six moment model follow the theoretical

Table I
Calculated values for $x_{2,crit}$ for various mixtures.

Mixture	m_2/m_1	Four moment model	Six moment model
H ₂ + He	2.0	0.415	0.430
He + Ne	5.0	0.308	0.316
H ₂ + Ne	10.0	0.240	0.227
H ₂ + Ar	19.8	0.183	0.150
He + Xe	32.8	0.148	0.123
H ₂ + Xe	65.1	0.110	0.071

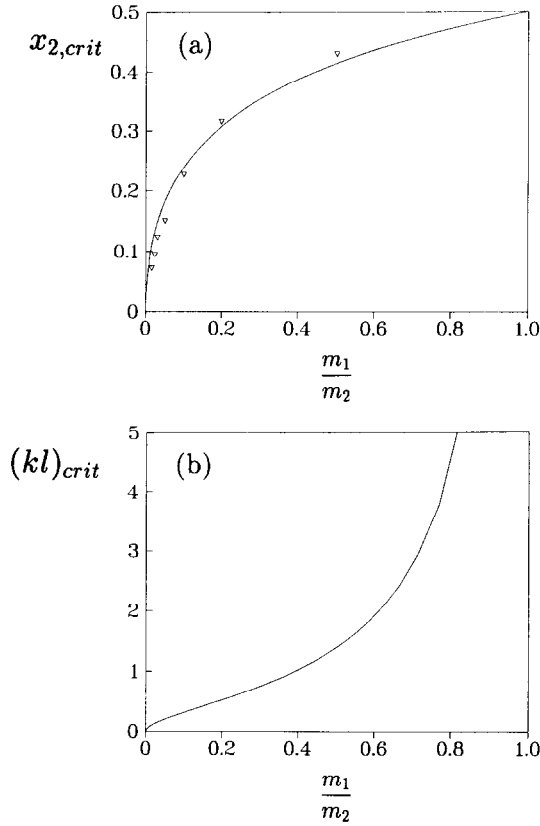


Fig. 4. (a) $x_{2,crit}$ versus m_1/m_2 for four moment (solid), six moment model (∇). (b) $(kl)_{crit}$ versus m_1/m_2 for four moment model (solid).

predictions of the four moment although for large mass ratios m_2/m_1 the differences between both model predictions increase. In fig. 4b the predictions for the critical reduced wavevector $(kl)_{crit}$ are shown only for the four moment model, since it is difficult to define a critical reduced wavevector in the six moment model. The value for $(kl)_{crit}$ decreases with increasing mass ratio m_2/m_1 . This means that decoupling already occurs at relatively long length scales for disparate mass mixtures.

3. Comparison with experimental results

We performed Rayleigh–Brillouin light scattering experiments on dilute $H_2 + Xe$ and $H_2 + Ar$ gas mixtures. The measurements were carried out at

room temperature ($T = 294$ K) and the pressure was varied in the range 1–50 bar. The plate spacing of the Fabry–Perot interferometer was 0.71 cm for one $H_2 + Xe$ mixture ($x_{Xe} = 0.02$) and 0.94 cm for all other mixtures. The spectra were fitted by a sum of Lorentzians in order to obtain the propagation frequencies, widths and amplitudes of the modes. One central Lorentzian (Rayleigh line) and two pairs of symmetrically shifted Lorentzians (Brillouin lines) were used in our fitting routine. Further details about the experimental setup and the fitting procedure can be found in ref. [8].

It was shown experimentally, by performing density- and wavevector-dependent measurements, that the phase velocity (ω/k) and the reduced wavevector kl (l is a characteristic length scale) are in fact the correct scaling parameters for the dispersion relation of dilute gas mixtures [22]. Since the present measurements were performed at constant wavevector ($k = 1.727 \times 10^7 \text{ m}^{-1}$), the data will be plotted as \tilde{z} ($= z/Wk$) versus kl , instead of the usual way of plotting dispersion relations, as in figs. 1–3. The reference length scale l is calculated using eqs. (8), (15) and (16),

$$l = \frac{\mu DW}{k_B T_0}, \tag{44}$$

and the experimental value for the diffusion coefficient D (table II). It is assumed that D varies inversely proportional with pressure, where the value at $p = 1$ bar is used as reference.

The length scale l differs from the characteristic length scale we used in previous publications: the effective mean free path. The effective mean free path was calculated using the persistence of velocities, which does not appear explicitly in the present theory. Using this characteristic length scale we were able to scale the dispersion of the slow sound mode of various mixtures onto a single curve [8].

Our experimental results will only be compared with the six moment model. Although the four moment model is very useful in studying many aspects of the dispersion relation analytically, it does not give the correct hydrodynamic limit for the sound modes. Therefore, only the six moment model will be considered.

Table II
Parameters used to calculate $\tilde{z} = z/Wk$ and $kl = Wk/\nu$ ($T = 294$ K). The diffusion coefficients ($T = 300$ K, $p = 1$ bar) are obtained from ref. [23].

Mixture	m_2/m_1	D ($10^{-4} \text{ m}^2\text{s}^{-1}$)	W (m s^{-1})	ν (10^9 s^{-1})
$H_2 + Xe$	65.1	0.6233	1568	19.7
$H_2 + Ar$	19.8	0.8240	1595	15.4

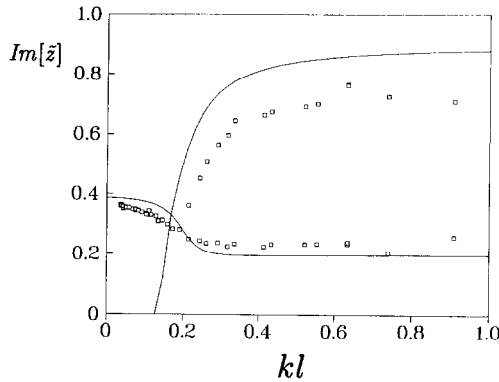


Fig. 5. Dispersion relation \tilde{z} ($= z/Wk$) versus kl for $H_2 + Ar$, $x_{Xe} = 0.23$. Six moment model (dashed), experimental (box).

In fig. 5 the results for a $H_2 + Ar$ mixture, $x_{Ar} = 0.23$, are shown. Considered the fact that there are no adjustable parameters, the agreement with the six moment model is satisfactory. For this mixture the agreement with kinetic calculations was also good [7]. Experimentally, it was already shown for various $He + Xe$ mixtures, that the slow sound mode propagates with a phase velocity ($= \omega/k$) close to the adiabatic sound velocity of pure Xe [6]. In this case the phase velocity of the slow sound mode is close to $c_{S,Ar}$, the adiabatic sound velocity of pure Ar , while the phase velocity of the fast sound mode is somewhat smaller than c_{S,H_2} . This is also the case for $H_2 + Xe$ ($x_{Xe} = 0.17$), as is shown in fig. 6: the fast sound mode has a much smaller phase velocity than the adiabatic sound velocity of pure H_2 , the slow sound mode however has a phase velocity close to the sound velocity in pure Xe . The agreement with the six moment model is less convincing for this mixture, experimentally the

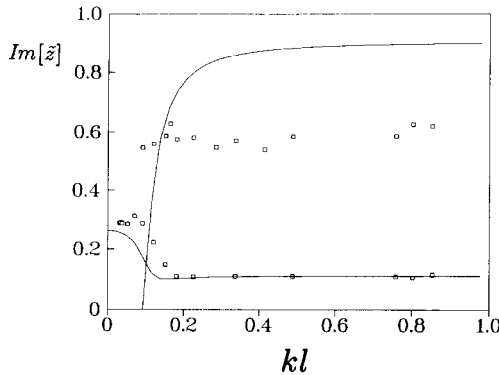


Fig. 6. As fig. 5 for $H_2 + Xe$, $x_{Xe} = 0.17$.

transition from hydrodynamic sound to slow sound takes place at somewhat larger values of kl . This may be related to the fact that the composition is already close to the critical composition (the model predictions change dramatically in the vicinity of the ‘critical point’). The agreement with another $H_2 + Xe$ mixture ($x_{Xe} = 0.33$) is reasonable, however (fig. 7). Due to the relatively high Xe-concentration, no fast sound mode could be observed for this mixture [8,9].

To our knowledge there are no experimental results in which hydrodynamic sound becomes a fast propagating mode at present. According to the predictions of the six moment model, this can be observed in $H_2 + Xe$ mixtures with $x_{Xe} < 0.071$. Therefore, we have studied a $H_2 + Xe$ mixture with a very low Xe-concentration ($x_{Xe} = 0.02$). Some typical experimental light scattering spectra ($I(k, \omega)$) are shown in fig. 8a. As can be seen in the spectra the peak position of the strongly damped Brillouin line shifts to higher frequencies as kl is increased. This can be observed in more detail in the spectrum of $\omega^2 I(k, \omega)$ (fig. 8b), which is proportional to the longitudinal current autocorrelation function. In fig. 9 the corresponding dispersion relation is shown. At the highest pressure ($p = 20$ bar) the hydrodynamic regime is apparently not yet reached. The phase velocity of the sound mode differs considerably from the calculated sound velocity of the mixture, which indicates that deviations from hydrodynamic behaviour start at even higher pressures (smaller values of kl). The phase velocity of the fast mode however is close to the adiabatic sound velocity of pure H_2 .

It is shown that for $H_2 + Xe$ mixtures with a relative large Xe-concentration ($x_{Xe} = 0.17, 0.03$) the extension of hydrodynamic sound is the slow sound mode. For the mixture with the low Xe-concentration ($x_{Xe} = 0.02$) the extension of hydrodynamic sound is a fast propagating mode. This is in

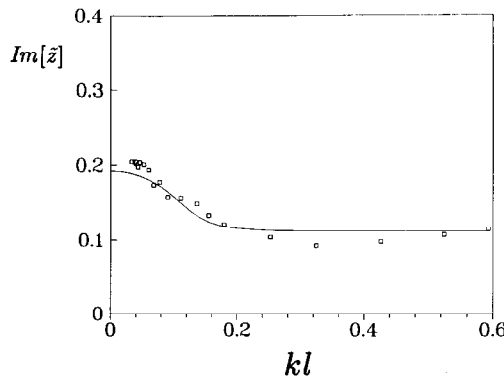


Fig. 7. As fig. 5 for $H_2 + Xe$, $x_{Xe} = 0.33$.

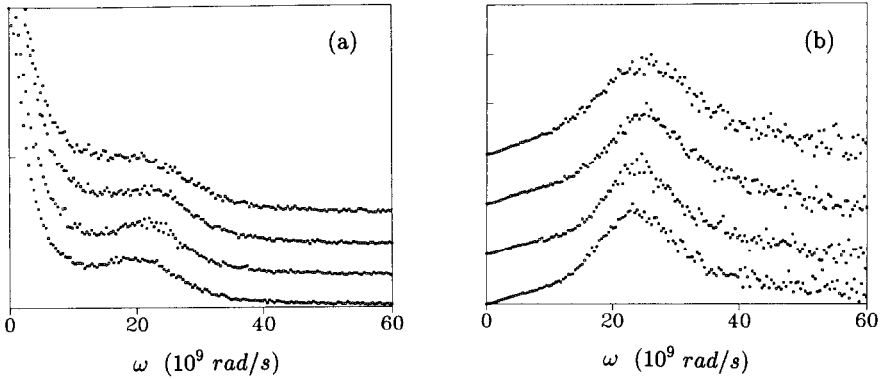


Fig. 8. (a) Experimental light scattering spectra $I(k, \omega)$ (a.u.) versus ω for $H_2 + Xe$, $x_{Xe} = 0.02$. From top to bottom $p = 3.0$ bar, $kl = 0.14$; $p = 5.5$ bar, $kl = 0.075$; $p = 12.8$ bar, $kl = 0.0325$; $p = 21.8$ bar, $kl = 0.0192$. (b) Corresponding current autocorrelation functions $\omega^2 I(k, \omega)$ (a.u.) versus ω .

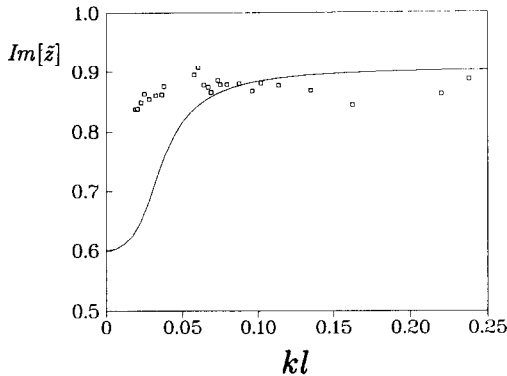


Fig. 9. As fig. 5 for $H_2 + Xe$, $x_{Xe} = 0.02$.

qualitative agreement with the prediction of the six-moment model; $x_{Xe,crit} = 0.071$. The present results for $H_2 + Xe$ give a strong indication for the existence of a critical composition.

4. Discussion

Fast and slow sound seems to be a general feature of the dynamics of disparate mass mixtures [1–10]. This suggests that the dynamic decoupling of the sound modes is primarily related to a high mass ratio. This may justify the use of a simplified two-temperature model for qualitative purposes. In this

simplified model, dissipation is only due to the coupling of the velocity fields and the species temperatures. We find some interesting features of this model such as a critical composition and the occurrence of sound propagation gaps. In the four moment model the critical composition can be obtained analytically. The critical composition demarcates the composition ranges where the light or the heavy component dominates the dynamics of the mixture. If we now consider the ratio of the momentum densities of both species, and assume that the flow velocity u_i is proportional with the thermal velocity ($=\sqrt{k_B T_0/m_i}$) [15,24],

$$\frac{\rho_1 u_1}{\rho_2 u_2} = \frac{1-x_2}{x_2} \delta . \quad (45)$$

The momentum densities balance at $x_2 = \delta/(1 + \delta)$, which is precisely the critical composition that is predicted by the four moment model. Apparently it is the ratio of the momentum densities that determines whether the extension of the hydrodynamic sound mode is the fast or the slow propagating mode. Inclusion of the species temperatures (6 moment model) results in slightly different values for the critical composition (table I).

At this stage it is interesting to consider the ultrasonic experiments on dilute He + Xe mixtures [11]. In the ultrasonic case the wavevector (complex) is measured as a function of frequency (real), contrary to the light-scattering case where frequency (complex) is measured as a function of wavevector (real). The four moment model predicts, for the ultrasonic case, a critical point at $(\omega/\nu)_{\text{crit}} = \delta^2/(1 - \delta^4)$ and $x_{2,\text{crit}} = 0.5$. At large frequencies $(\omega/\nu) \gg (\omega/\nu)_{\text{crit}}$ two sound modes are predicted. Due to the large absorption of the ultrasonic waves at low densities, only one (forced) sound mode could be observed experimentally. The ten moment model predicts a critical composition $x_{2,\text{crit}} = 0.540$, which is only slightly different from the four moment model result. For hard sphere mixtures it was found that the two-temperature model predicts $0.5 < x_{2,\text{crit}} < 0.6$ for $m_2/m_1 > 5$ [12]. Experimentally the critical point occurs at $x_{2,\text{crit}} \approx 0.5$. Using the same approximations as in the previous paragraph we find that the ratio of the kinetic energy densities is

$$\frac{\rho_1 u_1^2}{\rho_2 u_2^2} = \frac{1-x_2}{x_2} . \quad (46)$$

This ratio equals 1 when the number densities balance, $x_2 = 0.5$. This may indicate that in ultrasonic experiments the dynamics are governed by kinetic energy densities or number densities. The connection between the eigenmodes

as measured by light scattering and forced modes as measured by ultrasonic experiments is still unclear [4].

The basic feature of the four moment model is the coupling between the light and heavy species, which is a friction term that acts on the velocity difference w (eq. (20)). The scaling parameter kl represents the ratio of an ‘elastic force’ and a ‘friction force’:

$$kl = \frac{Wk}{An_0(m_1 + m_2)}, \quad (47)$$

so the $kl \rightarrow 0$ limit corresponds to the long wavelength limit as well as to the strong coupling limit. In the following intuitive reasoning only propagating modes will be considered. Due to the strong coupling between the velocity fields u_1 and u_2 , there is no relative motion between both subsystems in the $kl \rightarrow 0$ limit. So in this limit a collective sound wave can propagate through the mixture. In the short wavelength limit ($kl \rightarrow \infty$), or the weak coupling limit, both the velocity fields u_1 and u_2 are decoupled and sound waves can propagate independently through the light and heavy species. If $kl \sim 1$ the elastic force and friction force are of comparable magnitude. In this kl -regime the dynamics of both subsystems decouple and even a sound propagation gap can occur. The mass ratio is an important parameter: for large mass ratios m_2/m_1 dynamic decoupling takes place at relatively low values of kl (fig. 4b).

Campa and Cohen [26] have shown that the temperature–temperature correlation function $S_{ii}^T(k, \omega)$ exhibits a clearly resolved slow sound peak whereas the density–density correlation function $S_{ii}(k, \omega)$ does not. Although this is a useful tool in theoretical studies, $S_{ii}^T(k, \omega)$ cannot be measured experimentally. The current–current correlation function, which is proportional to $\omega^2 S(k, \omega)$, can be determined experimentally and gives better resolved fast and slow sound peaks than $S(k, \omega)$ [7–9].

If higher moments such as heat flux and pressure tensor are included (i.e. the 10 moment model), similar results for the critical features of the dispersion relation are obtained. For example, for a mass ratio $m_2/m_1 = 19.8$ ($H_2 + Ar$), the ten moment model predicts a critical composition $x_{Ar, crit} \approx 0.12$. Kinetic calculations [4] on the same system show that this composition is $0.1 < x_{Ar, crit} < 0.2$.

An interesting feature of the present theory is the continuation of the hydrodynamic sound mode in a fast propagating mode. To our knowledge this is not predicted by any hydrodynamic theory. Continuation of the hydrodynamic mode in a slow propagating mode is predicted by the simplified hydrodynamic model [20]. The light-scattering experiments of Baharudin [25] on a dilute He + Kr mixture ($x_{Kr} = 0.61$) confirm this theory. For disparate

mass gas mixtures, the simplified hydrodynamic model predicts that in the ‘isoconcentration limit’ (large k), the phase velocity of the extended sound mode is very close to adiabatic sound velocity of the heavy component. The phase velocity of the extension of the hydrodynamic mode (large kl) is also within 2% equal to the adiabatic Kr sound velocity, which is consistent with the predictions of the six moment model.

Westerhuijs et al. [27] have performed neutron scattering experiments on a He + Ne mixture ($x_{\text{Ne}} = 0.35$). They have proposed a model using the Zwanzig–Mori operator formalism and fitted this model to the neutron scattering spectra. The five basic variables of this model are the microscopic densities and longitudinal velocities of both species and the microscopic energy density. Extrapolation of the fitting results to the limit $k \rightarrow 0$ gave the correct adiabatic sound velocity of the mixture and showed that the slow sound mode is the extension of the hydrodynamic sound mode at large wavevectors. The theoretical prediction of the six moment model for a dilute He + Ne mixture is $x_{\text{Ne,crit}} = 0.306$. It would be interesting to see whether a critical composition can also be determined using neutron scattering data of dense binary mixtures.

5. Conclusion

A simplified version of the two-temperature model for gas mixtures, the four moment model, predicts the existence of a critical composition $x_{2,\text{crit}}$ that demarcates two dynamic regions. For $x_2 > x_{2,\text{crit}}$ the hydrodynamic sound mode becomes a slow propagating mode and for $x_2 < x_{2,\text{crit}}$ the hydrodynamic sound mode becomes a fast propagating mode for large reduced wavevectors. These dynamic regions are characterized by domination of the light or heavy component momentum density. The four moment model is useful in studying many aspects of the dispersion relation analytically, but it does not give the correct hydrodynamic limit for the sound modes due to neglect of the temperature fluctuations. Therefore, our experimental results were only compared with the six moment model which has similar critical features as the four moment model and furthermore predicts the correct phase velocity for the hydrodynamic sound mode.

The existence of a critical composition is confirmed experimentally for the $\text{H}_2 + \text{Xe}$ system. For $x_{\text{Xe}} = 0.17$ and 0.33, the continuation of the hydrodynamic sound mode is the slow sound mode which propagates with a phase velocity close to the adiabatic sound velocity of pure Xe. It was also found that, for $x_{\text{Xe}} = 0.02$, the extension of the hydrodynamic sound mode is a fast mode which propagates with a phase velocity close to the adiabatic sound

velocity of pure H₂. These findings qualitatively confirm the predictions of the six moment model; the critical composition for H₂ + Xe equals $x_{\text{Xe,crit}} = 0.071$.

Acknowledgement

The authors wish to thank A. Bot for critically reading the manuscript and H.M. Schaink for bringing the sound propagation gaps to our attention. This work is part of the scientific program of the Foundation for Fundamental research of Matter (FOM).

References

- [1] J. Bosse, G. Jacucci, M. Ronchetti and W. Schirmacher, *Phys. Rev. Lett.* 57 (1986) 3277.
- [2] A. Campa and E.G.D. Cohen, *Phys. Rev. A* 39 (1989) 4909.
- [3] A. Campa and E.G.D. Cohen, *Phys. Rev. Lett.* 61 (1988) 853.
- [4] A. Campa and E.G.D. Cohen, *Phys. Rev. A* 41 (1990) 5451.
- [5] W. Montfrooij, P. Westerhuijs, V.O. de Haan and I.M. de Schepper, *Phys. Rev. Lett.* 63 (1989) 544.
- [6] G.H. Wegdam and H.M. Schaink, *Phys. Rev. A* 41 (1990) 3419.
- [7] G.H. Wegdam, A. Bot, R.P.C. Schram and H.M. Schaink, *Phys. Rev. Lett.* 63 (1989) 2697.
- [8] R.P.C. Schram, G.H. Wegdam and A. Bot, *Phys. Rev. A* 44 (1991) 8062.
- [9] R.P.C. Schram, A. Bot, H.M. Schaink and G.H. Wegdam, *J. Phys. Condens. Matter* 2 (1990) SA157.
- [10] M.J. Clouter, H. Luo, H. Kiefte and J.A. Zollweg, *Phys. Rev. A* 41 (1990) 2239.
- [11] J.R. Bowler and E.A. Johnson, *Proc. R. Soc. London A* 408 (1986) 79.
- [12] B. Kamgar-Parsi and E.G.D. Cohen, *Int. J. Thermophys.* 7 (1986) 395.
- [13] C.J. Goebel, S.M. Harris and E.A. Johnson, *Phys. Fluids* 19 (1976) 627.
- [14] I.M. de Schepper, J.C. van Rijs and E.G.D. Cohen, *Physica A* 134 (1985) 1.
- [15] G.H. Wegdam and H.M. Schaink, *Mol. Phys.* 65 (1988) 531.
- [16] R.J. Huck and E.A. Johnson, *Phys. Rev. Lett.* 44 (1980) 142.
- [17] J.M. Burgers, *Flow equations for Composite Gases* (Academic Press, New York, 1969).
- [18] A. Campa and E.G.D. Cohen, in: *Kinetic Theory and Extended Thermodynamics*, I. Muller and T. Ruggeri, eds. (Pitagora Editrice, Bologna, Italy, 1987) p. 79.
- [19] M.J. Zuilhof, E.G.D. Cohen and I.M. de Schepper, *Phys. Lett. A* 103 (1984) 120.
- [20] W.S. Gornall and C.S. Wang, *J. Phys. (France) C1* 33 (1972) 51.
- [21] H.N.W. Lekkerkerker and J.P. Boon, *Phys. Lett. A* 39 (1972) 9.
- [22] G.H. Wegdam and H.M. Schaink, *Phys. Rev. A* 40 (1989) 7301.
- [23] P.J. Dunlop, H.L. Robjohns and C.M. Bignell, *J. Chem. Phys.* 86 (1987) 2922.
- [24] H.M. Schaink, Ph.D. thesis, University of Amsterdam (1989).
- [25] B.Y. Baharudin, P.E. Schoen and D.A. Jackson, *Phys. Lett. A* 42 (1972) 77.
- [26] A. Campa and E.G.D. Cohen, *Physica A* 174 (1991) 214.
- [27] P. Westerhuijs, W. Montfrooij, L.A. de Graaf and I.M. de Schepper, *Phys. Rev. A* 45 (1992) 3749.